



Glucocorticoids Reprogram β -Cell Signaling to Preserve Insulin Secretion

Nicholas H.F. Fine,^{1,2} Craig L. Doig,^{1,2} Yasir S. Elhassan,^{1,2} Nicholas C. Vierra,³ Piero Marchetti,⁴ Marco Bugliani,⁴ Rita Nano,⁵ Lorenzo Piemonti,⁵ Guy A. Rutter,⁶ David A. Jacobson,³ Gareth G. Lavery,^{1,2} and David J. Hodson^{1,2,7}

Diabetes 2018;67:278–290 | <https://doi.org/10.2337/db16-1356>

Excessive glucocorticoid exposure has been shown to be deleterious for pancreatic β -cell function and insulin release. However, glucocorticoids at physiological levels are essential for many homeostatic processes, including glycemic control. We show that corticosterone and cortisol and their less active precursors 11-dehydrocorticosterone (11-DHC) and cortisone suppress voltage-dependent Ca^{2+} channel function and Ca^{2+} fluxes in rodent as well as in human β -cells. However, insulin secretion, maximal ATP/ADP responses to glucose, and β -cell identity were all unaffected. Further examination revealed the upregulation of parallel amplifying cAMP signals and an increase in the number of membrane-docked insulin secretory granules. Effects of 11-DHC could be prevented by lipotoxicity and were associated with paracrine regulation of glucocorticoid activity because global deletion of 11 β -hydroxysteroid dehydrogenase type 1 normalized Ca^{2+} and cAMP responses. Thus, we have identified an enzymatically amplified feedback loop whereby glucocorticoids boost cAMP to maintain insulin secretion in the face of perturbed ionic signals. Failure of this protective mechanism may contribute to diabetes in states of glucocorticoid excess, such as Cushing syndrome, which are associated with frank dyslipidemia.

Circulating glucocorticoids exert potent metabolic effects, including lipolysis, hepatic gluconeogenesis, amino acid mobilization, and reduced skeletal muscle glucose uptake

(1). This is facilitated by the enzyme 11 β -hydroxysteroid dehydrogenase type 1 (HSD11B1), which (re)activates glucocorticoid in a tissue-specific manner to determine bioavailability (2). As such, states of glucocorticoid excess (e.g., Cushing syndrome) are prodiabetic because they cause profound glucose intolerance and insulin resistance.

Although systemic administration of glucocorticoids induces a compensatory increase in β -cell mass and eventually insulin secretory failure as a result of insulin resistance (3), effects directly on β -cell function are less well understood. Suggesting an important link between glucocorticoids and insulin release, β -cell-specific glucocorticoid receptor (GR) overexpression reduces glucose tolerance (4). However, *in vitro* studies that used isolated islets have shown inhibitory or no effect of glucocorticoids on glucose-stimulated insulin secretion, depending on the steroid potency, concentration, and treatment duration (5–9). By contrast, HSD11B1 increases ligand availability at the GR by converting less-active to more active glucocorticoid (11-dehydrocorticosterone (11-DHC)→corticosterone in rodents; cortisone→cortisol in man), impairing β -cell function in islets both *in vitro* and *in vivo* (6,10,11). Whereas 11-DHC has consistently been shown to impair β -cell function in islets from obese animals, conflicting reports exist about its effects on normal islets (7,10).

More generally, the signaling components targeted by glucocorticoids are not well defined. Although exogenous application of glucocorticoid subtly decreases insulin release

¹Institute of Metabolism and Systems Research, University of Birmingham, Edgbaston, U.K.

²Centre for Endocrinology, Diabetes and Metabolism, Birmingham Health Partners, Birmingham, U.K.

³Department of Molecular Physiology and Biophysics, Vanderbilt University, Nashville, TN

⁴Department of Clinical and Experimental Medicine, University of Pisa, Pisa, Italy

⁵Diabetes Research Institute, San Raffaele Scientific Institute, Milan, Italy

⁶Section of Cell Biology and Functional Genomics, Department of Medicine, Imperial College London, London, U.K.

⁷Centre of Membrane Proteins and Receptors, University of Birmingham and University of Nottingham, Midlands, U.K.

Corresponding author: David J. Hodson, d.hodson@bham.ac.uk.

Received 5 November 2016 and accepted 16 November 2017.

This article contains Supplementary Data online at <http://diabetes.diabetesjournals.org/lookup/suppl/doi:10.2337/db16-1356/-/DC1>.

© 2017 by the American Diabetes Association. Readers may use this article as long as the work is properly cited, the use is educational and not for profit, and the work is not altered. More information is available at <http://www.diabetesjournals.org/content/license>.

and NADP, cAMP, and inositol phosphate production (5), these studies were performed by using high-dose dexamethasone (25× relative potency compared with cortisol). Conversely, administration of the same glucocorticoid in drinking water augments insulin release by increasing the number of docked exocytotic vesicles as well as β -cell mitochondrial potential/metabolism (12). However, indirect effects of insulin resistance cannot be excluded because studies in high-fat diet-fed mice have shown that compensatory β -cell responses, including proliferation, occur within a few days (13). Furthermore, glucocorticoid administration or GR deletion in the early neonatal period alters β -cell development, leading to reductions in the expression of key maturity markers, including Pdx1, Nkx6.1, and Pax6 (14,15). Whether this is also seen in adult islets, as may occur during diabetes (16), is unknown.

In the current study, we investigated the mechanisms by which the endogenous glucocorticoids corticosterone and cortisol affect β -cell function. By using in situ imaging approaches together with biosensors, we reveal that glucocorticoids perturb cytosolic Ca^{2+} concentration through effects on voltage-dependent Ca^{2+} channel (VDCC) function without altering β -cell maturity, glucose-induced changes in the ATP/ADP ratio, or incretin responsiveness. This, however, does not reduce insulin secretion because glucocorticoids upregulate parallel cAMP signaling pathways. The less-active glucocorticoids 11-DHC and cortisone show identical effects, which could be reversed in mouse after global deletion of *Hsd11b1*. Thus, a steroid-regulated feedback loop encompassing an enzymatic amplification step maintains normal insulin secretory output in the face of impaired β -cell ionic fluxes.

RESEARCH DESIGN AND METHODS

Animals

CD1 mice (8–12 weeks old, male) were used as wild-type tissue donors. *Hsd11b1*^{-/-} mice were generated as previously described (17). Studies were regulated by the Animals (Scientific Procedures) Act 1986 of the U.K., and approval was granted by the University of Birmingham's Animal Welfare and Ethical Review Body.

Islet Isolation

Islets were isolated by using collagenase digestion and cultured in RPMI medium supplemented with 10% FCS, 100 units/mL penicillin, and 100 $\mu\text{g}/\text{mL}$ streptomycin. Vehicle (ethanol 0.2%), 11-DHC (20/200 nmol/L), or corticosterone (20 nmol/L) (i.e., within the circulating free glucocorticoid range) were applied for 48 h. BSA-conjugated palmitate was applied at 0.5 mmol/L.

Human Islet Culture

Islets were obtained from isolation centers in Alberta (Alberta Diabetes Institute IsletCore), Canada (18), and Pisa and Milan, Italy, with local and national ethical permission. Islets were cultured in RPMI medium containing 10% FCS, 100 units/mL penicillin, 100 $\mu\text{g}/\text{mL}$ streptomycin, and 0.25 $\mu\text{g}/\text{mL}$ fungizone; supplemented with 5.5 mmol/L D-glucose; and treated with either vehicle

(ethanol 0.2%), cortisone (200 nmol/L), or cortisol (20 nmol/L) for 48 h. See Supplementary Table 1 for donor characteristics. Studies were approved by the National Research Ethics Committee (REC reference 16/NE/0107, Newcastle and North Tyneside, U.K.).

Calcium, ATP/ADP, and cAMP Imaging

Islets were loaded with 10 $\mu\text{mol}/\text{L}$ Fluo8 AM for 45 min at 37°C before washing and incubation in buffer for another 30 min to allow cleavage by intracellular esterase. Imaging was conducted by using either 1) a CrestOptics X-Light spinning disk and 10×/0.4 numerical aperture (NA) objective or 2) a Zeiss LSM 780 confocal microscope and 10×/0.45 NA objective. For the CrestOptics system, excitation was delivered at $\lambda = 458\text{--}482$ nm (400-ms exposure, 0.33 Hz) and emitted signals detected at $\lambda = 500\text{--}550$ nm by using an electron-multiplying charge-coupled device (Photometrics). For the Zeiss system, excitation was delivered at $\lambda = 488$ nm and emitted signals detected at $\lambda = 499\text{--}578$ nm by using a photomultiplier tube. Fura2 was loaded as for Fluo8, and imaging was performed by using light-emitting diodes (excitation $\lambda = 340/385$ nm, emission $\lambda = 470\text{--}550$ nm).

ATP/ADP ratios and cAMP responses were measured by using adenovirus harboring either Perceval (excitation/emission as for Fluo8) or the fluorescence resonance energy transfer (FRET) probe, exchange protein directly activated by cAMP 2 (Epac2)-camps (excitation $\lambda = 430\text{--}450$ nm; emission $\lambda = 460\text{--}500$ nm and 520–550 nm) (19,20). For Perceval, glucose was increased from 3 to 11 mmol/L, which leads to plateau responses (21). An effect of glucocorticoid on Epac2-camps expression was unlikely because single- and dual-channel fluorescence under maximal stimulation was similar for all treatments (Supplementary Table 2). In all cases, HEPES-bicarbonate buffer was used, containing (in mmol/L) 120 NaCl, 4.8 KCl, 24 NaHCO₃, 0.5 Na₂HPO₄, 5 HEPES, 2.5 CaCl₂, 1.2 MgCl₂, and 3–17 D-glucose. Ca^{2+} , cAMP, and ATP/ADP traces were normalized as F / F_{min} , where F is fluorescence at any given time point and F_{min} is minimum fluorescence during the recording (i.e., under basal conditions).

Electrophysiology

VDCC currents were recorded from dispersed mouse β -cells as previously described (22). Patch electrodes were pulled to a resistance of 3–4 M Ω then filled with an intracellular solution containing (in mmol/L) 125 CsCl, 10 tetraethylammonium Cl, 1 MgCl₂, 5 EGTA, 10 HEPES, 3 MgATP, pH 7.22 with CsOH. Cells were patched in HEPES-buffered solution + 17 mmol/L glucose. Upon obtaining the whole-cell configuration with a seal resistance >1 G Ω , the bath solution was exchanged for a modified HEPES-buffered solution containing (in mmol/L) 62 NaCl, 20 tetraethylammonium Cl, 30 CaCl₂, 1 MgCl₂, 5 CsCl, 10 HEPES, 17 glucose, 0.1 tolbutamide, pH 7.35 with NaOH. β -Cells were perfused for 3 min with this solution before initiating the VDCC recording protocol. Voltage steps of 10 mV were applied from a holding potential of -80 mV; linear leak currents were subtracted online by using a P/4 protocol. Data were analyzed by using Clampfit software (Molecular Devices).

Immunohistochemistry and Superresolution Imaging

Islets were fixed overnight at 4°C in 4% formaldehyde before immunostaining with rabbit monoclonal anti-insulin (1:400; Cell Signaling Technology) and goat anti-rabbit Alexa Fluor 568 (1:1,000). Superresolution imaging was performed by using a VT-iSIM system (VisiTech International) and 100 \times /1.49 NA objective. Excitation was delivered at $\lambda = 561$ nm, and emitted signals were captured at $\lambda = 633$ – 647 nm by using an sCMOS camera. Image stacks were cropped to include only the near-membrane regions and exclude out-of-focus signal and converted to 8-bit gray scale before obtaining the maximum intensity projection. Auto thresholding was performed in Fiji (National Institutes of Health) to produce a binary snapshot from which the area occupied by insulin granules could be quantified as a unitary ratio (V/v) versus the total membrane area by using the analyze particle plug-in as previously described (20).

Real-time PCR

Relative mRNA abundance was determined by using SYBR Green chemistry, and fold change in mRNA expression was calculated compared with *Actb* by using the $2^{-\Delta\Delta Ct}$ method (see Supplementary Table 3 for primer sequences). *Hsd11b1* mRNA abundance was determined by using TaqMan assays for mouse (cat. #4331182) and human (cat. #4331182) tissue. *Hsd11b1* expression was calculated by using $2^{-\Delta Ct} \times 1,000$, and transformed values are presented as arbitrary units.

Measurements of Insulin Secretion and ATP in Isolated Islets

Batches of eight islets were placed in low-bind Eppendorf tubes and incubated for 30 min at 37°C in HEPES-bicarbonate buffer containing 3 mmol/L glucose before the addition of either 3 mmol/L glucose, 17 mmol/L glucose, or 17 mmol/L glucose + 10 mmol/L KCl for another 30 min and collection of supernatant. Total insulin was extracted into acid ethanol. Insulin concentration was determined by using an HTRF (homogeneous time-resolved fluorescence)-based assay (Cisbio) according to the manufacturer's instructions. Total ATP at 3 and 17 mmol/L glucose was measured in batches of 25 islets by using a luciferase-based assay (Invitrogen), and values were normalized to total protein.

Statistical Analyses

Pairwise comparisons were performed with paired or unpaired Student *t* test. Interactions among multiple treatments were determined by one-way ANOVA (adjusted for repeated measures as necessary) followed by Bonferroni or Tukey post hoc test. Analyses were conducted by using GraphPad Prism and Igor Pro software.

RESULTS

Glucocorticoids Alter Ionic but Not Metabolic Fluxes

Fluo8-loaded β -cells residing within intact islets of Langerhans were subjected to multicellular Ca^{2+} imaging approaches (23). Individual β -cells responded to elevated glucose (3 mmol/L \rightarrow 17 mmol/L) with large increases in cytosolic Ca^{2+} levels (Fig. 1A and B). Whereas 11-DHC 20 nmol/L was

without effect, higher (200 nmol/L) concentrations suppressed the amplitude and area under the curve (AUC) of Ca^{2+} rises in response to glucose and glucose + 10 mmol/L KCl by $\sim 30\%$ (Fig. 1A–E and Supplementary Figs. 1A and B and 2A–C), and this reached $\sim 50\%$ in the presence of corticosterone 20 nmol/L. Results were confirmed by using the ratiometric Ca^{2+} indicator Fura2, excluding a major contribution of basal Ca^{2+} levels to the magnitude changes detected here (Supplementary Fig. 2A–C). No effect of glucocorticoid on the time to onset of Ca^{2+} rises was detected (lag period \pm SD 22.5 ± 7.7 vs. 26.3 ± 9.7 vs. 24.0 ± 6.2 s for control, 11-DHC, and corticosterone, respectively; nonsignificant by one-way ANOVA). The peak Ca^{2+} response to KCl depolarization in low (3 mmol/L) glucose was unaffected by 11-DHC and significantly increased by corticosterone (Supplementary Fig. 2D and E), although both glucocorticoids reduced Ca^{2+} amplitude when KCl concentration was increased from 10 to 30 mmol/L (24) (Supplementary Fig. 2F and G). Although both 11-DHC and corticosterone led to more sustained Ca^{2+} influx in response to 3 mmol/L glucose + 10 mmol/L KCl (Supplementary Fig. 2E), this was not the case with 30 mmol/L KCl (Supplementary Fig. 2G). An effect of treatment on basal Ca^{2+} levels at 3 mmol/L glucose was unlikely because the Fura2 340/385 ratio was not significantly affected by 11-DHC or corticosterone (Supplementary Fig. 2H).

Supporting an action on later steps in ionic flux generation, 11-DHC and corticosterone reduced Ca^{2+} oscillation frequency at a moderately (11 mmol/L) elevated glucose concentration (Fig. 1F and G). Glucocorticoids (cortisone and cortisol) also suppressed Ca^{2+} responses to glucose and glucose + 10 mmol/L KCl in human islets (Fig. 1H–J), without significantly altering basal Ca^{2+} concentration (Supplementary Table 4). The reported glucocorticoid actions were specific to glucose because both 11-DHC and corticosterone were unable to influence Ca^{2+} responses to exendin-4 in mouse islets in terms of oscillation frequency and AUC (Fig. 1K–M), these parameters being the primary drivers of incretin-stimulated Ca^{2+} fluxes in this species (23).

β -Cells Remain Differentiated in the Presence of Glucocorticoids

Immature or dedifferentiated β -cells fail to respond properly to glucose, a defect that can be partly explained by lowered transcription factor expression and impairments in metabolism and Ca^{2+} flux generation (25). This was unlikely to be the case here, however, because 11-DHC and corticosterone did not significantly affect mRNA abundance of the key β -cell maturity markers *Pdx1* (Fig. 2A–C) and *Nkx6.1* (Fig. 2D–F). Moreover, maximal ATP/ADP increases in response to glucose, measured by using the biosensor Perceval (26), were not significantly different (Fig. 2G and H). 11-DHC and corticosterone did not affect the time to onset (Supplementary Fig. 3A) or the amplitude (Supplementary Fig. 3B) of the initial, transient decrease in ATP/ADP. No significant effects of glucocorticoid on basal

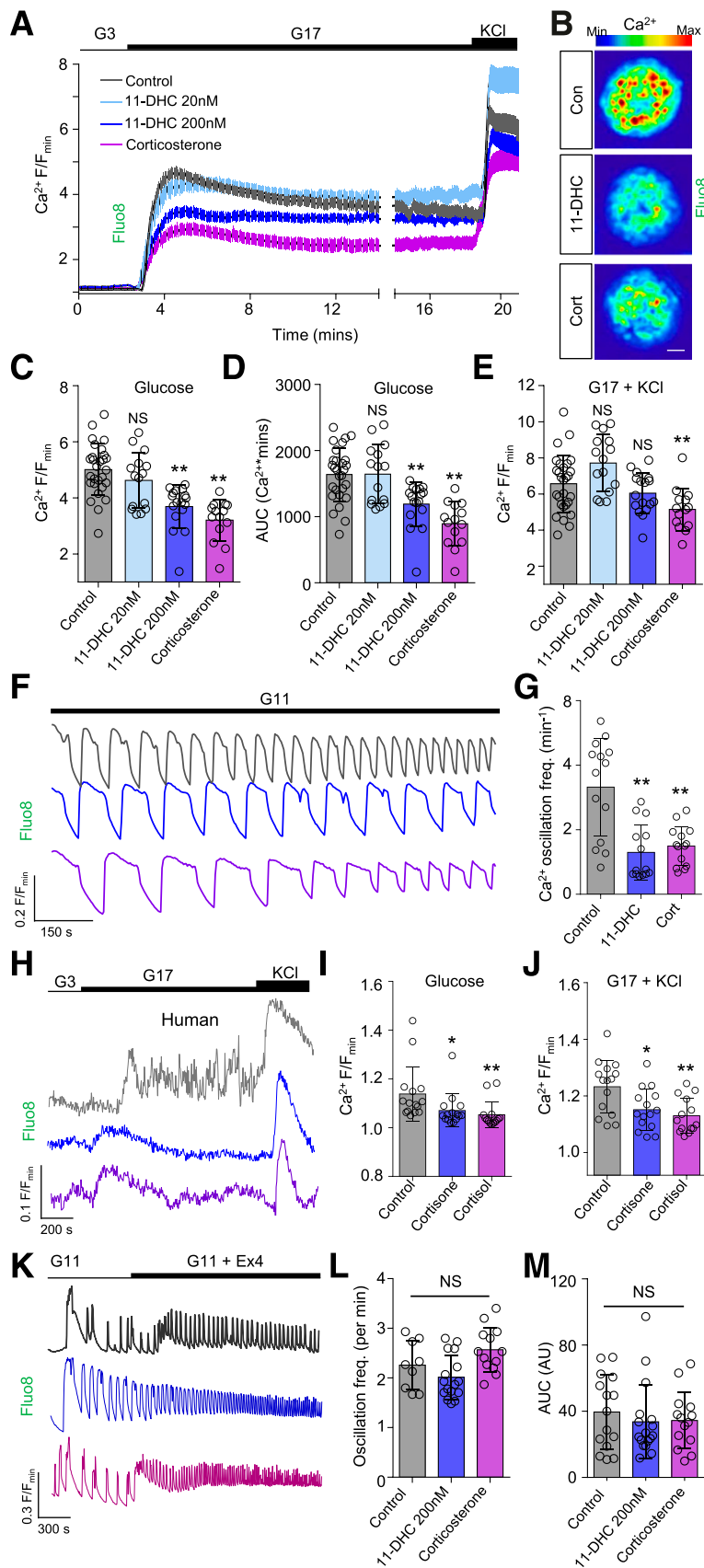


Figure 1—Glucocorticoids suppress cytosolic Ca^{2+} fluxes in response to glucose and glucose + KCl. **A**: Mean \pm SEM intensity-over-time traces showing glucose- and glucose + KCl-stimulated Ca^{2+} rises in mouse islets treated for 48 h with 11-DHC or corticosterone ($n = 14\text{--}28$ islets from six animals). **B**: Representative maximum intensity projection images showing impaired Ca^{2+} signaling in glucose-stimulated islets treated with

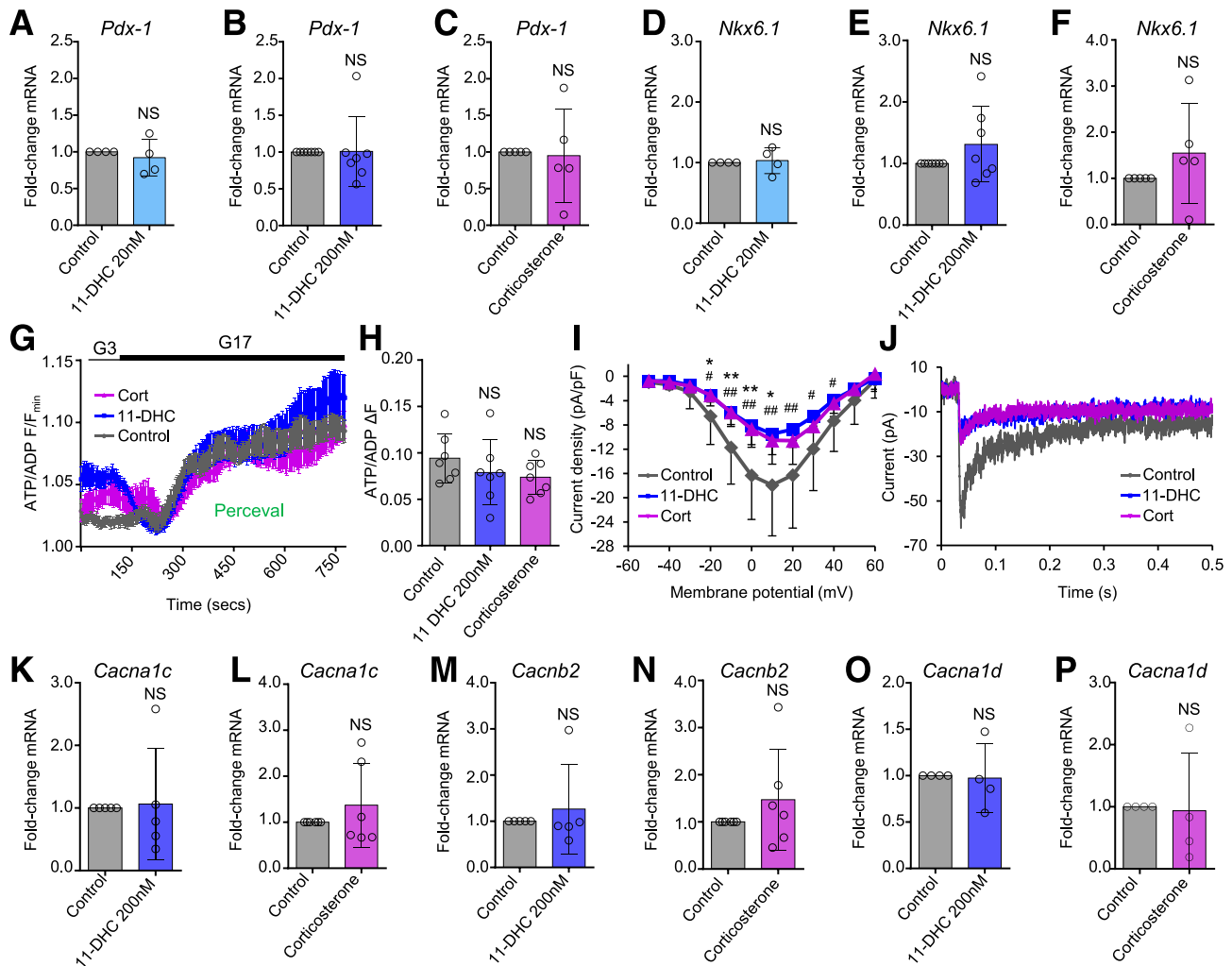


Figure 2—Glucocorticoids impair VDCC function despite preserved β -cell identity and metabolism. *A–F*: Expression of mRNA for the β -cell maturity markers *Pdx-1* (*A–C*) and *Nkx6.1* (*D–F*) are similar in control and 11-DHC/corticosterone-treated islets ($n = 4–7$ animals, 48 h). *G*: Mean \pm SEM traces showing no effect of glucocorticoids on maximal ATP/ADP responses to glucose measured using the biosensor Perceval. *H*: As for *G*, but summary bar graph showing the amplitude of ATP/ADP rises ($n = 7$ islets from four animals). *I*: 11-DHC and corticosterone reduce VDCC conductance as shown by the voltage-current relationship ($n = 4$ animals). *J*: As for *I*, but representative Ca^{2+} current traces. *K–P*: Expression levels of the VDCC α/β -subunits *Cacna1c* (*K* and *L*), *Cacnb2* (*M* and *N*), and *Cacna1d* (*O* and *P*) are not significantly altered by 11-DHC or corticosterone ($n = 4–6$ animals, 48 h). Corticosterone was applied at 20 nmol/L for 48 h. Unless otherwise stated, data are mean \pm SD. * $P < 0.05$, ** $P < 0.01$ for 11-DHC vs. control; # $P < 0.05$, ### $P < 0.01$ for corticosterone vs. control (NS, nonsignificant) by Student *t* test, Student paired *t* test, or one-way ANOVA (Bonferroni post hoc test). Cort, corticosterone; G3, 3 mmol/L glucose; G17, 17 mmol/L glucose.

or glucose-stimulated ATP levels were detected by luciferase-based assays (Supplementary Fig. 4). Patch-clamp electrophysiology revealed abnormal VDCC function in the presence

of glucocorticoids, with voltage-current curves showing a marked reduction in Ca^{2+} conductance (Fig. 2*I* and *J*). Suggestive of changes in VDCC function rather than

control, 200 nmol/L of 11-DHC, and corticosterone (scale bar = 20 μ m) (images cropped to show a single islet). *C*: Summary bar graph showing a significant reduction in the amplitude of glucose-stimulated Ca^{2+} rises after treatment with either glucocorticoid ($n = 14–28$ islets from six animals). *D*: As for *C*, but AUC. *E*: As for *C*, but glucose + KCl. *F*: Corticosterone and 11-DHC significantly decrease Ca^{2+} spiking frequency at high glucose (representative traces shown) ($n = 14$ islets from three animals). *G*: As for *F*, but summary bar graph showing Ca^{2+} oscillations per minute. *H*: Cortisone 200 nmol/L and cortisol 20 nmol/L blunt glucose- and glucose + KCl-stimulated Ca^{2+} rises in human islets (representative traces shown) ($n = 15–18$ islets from three donors, 48 h). *I* and *J*: As for *H*, but summary bar graphs showing amplitude of Ca^{2+} responses to glucose (*I*) and glucose + KCl (*J*). *K*: 11-DHC and corticosterone do not affect Ca^{2+} responses to the incretin mimetic exendin-4 (Ex4) 10 nmol/L (representative traces shown) ($n = 14–17$ islets from three animals). *L* and *M*: As for *K*, but summary bar graphs showing oscillation frequency (*L*) and AUC (*M*). KCl was applied at 10 mmol/L. Corticosterone was applied at 20 nmol/L for 48 h. Traces in *F*, *H*, and *K* share the same F/F_{min} scale but are offset in the y-axis. Unless otherwise stated, data are mean \pm SD. * $P < 0.05$, ** $P < 0.01$ by one-way ANOVA (Bonferroni post hoc test). AU, arbitrary unit; Con, control; Cort, corticosterone; freq., frequency; G3, 3 mmol/L glucose; G11, 11 mmol/L glucose; G17, 17 mmol/L glucose; max, maximum; min, minimum; NS, nonsignificant.

expression, transcript levels of the major α - and β -subunits *Cacna1c* (Fig. 2K and L), *Cacnb2* (Fig. 2M and N), and *Cacna1d* (Fig. 2O and P) were not significantly altered.

Glucocorticoids Do Not Affect Insulin Secretory Responses

In response to glucose, increases in ATP/ADP ratios lead to closure of K_{ATP} channels, opening of VDCCs, and Ca^{2+} -dependent insulin secretion (27). Thus, perturbed cytosolic Ca^{2+} fluxes/levels generally translate to reductions in insulin secretory output (27). However, glucose and glucose + KCl-stimulated insulin release were not significantly different after 48-h exposure of islets to 11-DHC or corticosterone (Fig. 3A). This was not due to an increase in insulin expression because *Ins1* mRNA levels were similar in the presence of both glucocorticoids (Fig. 3B–D). Likewise, total insulin content was not significantly different between treatments under all stimulation conditions examined (Fig. 3E). Insulin secretion also was unaffected by cortisone and cortisol treatment in primary human islets (Fig. 3F and G and Supplementary Table 1).

cAMP Signals Are Upregulated by Glucocorticoids

Granule release competency can be increased by signals, including cAMP, which act directly upon protein kinase A (PKA) and Epac2 (28). By using the FRET probe Epac2-camps to dynamically report cytosolic cAMP (20), glucose induced a robust increase in levels of the nucleotide (Fig. 4A). Both 11-DHC and corticosterone upregulated cAMP responses to glucose by ~ 1.5 -fold (Fig. 4A–C). This appeared necessary for maintenance of secretory output because chemical inhibition of PKA significantly reduced glucose-stimulated insulin release in 11-DHC-treated islets (Fig. 4D). Indeed, more granules were present at the membrane in glucocorticoid-treated islets, which was revealed by using superresolution structured illumination microscopy (Fig. 4E and F). Similar results were seen in human islets, with cortisone and cortisol both augmenting cAMP responses to glucose (Fig. 4G and H). As for Ca^{2+} , the actions of glucocorticoid were glucose-specific because neither 11-DHC nor corticosterone altered cAMP responses to exendin-4 (Fig. 4I and J). Supporting a central role for adenylate cyclase (*Adcy*) in this effect, expression of *Adcy1* was increased by both glucocorticoids (Fig. 4K and L), and induction of lipotoxicity with palmitate (shown previously to lower *Adcy9* mRNA [29]) prevented glucocorticoid from augmenting cAMP responses to glucose (Fig. 4M and N).

Hsd11b1 Is Expressed in Islets of Langerhans

HSD11B1 is responsible for catalyzing the conversion of 11-DHC to corticosterone and is an important mechanism that determines local glucocorticoid activity (30). Expression of HSD11B1 in islets has been shown previously to be sufficient for 11-DHC \rightarrow corticosterone conversion (7). We therefore repeated studies in islets obtained from mice globally lacking one (*Hsd11b1*^{+/-}) or both (*Hsd11b1*^{-/-}) alleles of *Hsd11b1*. Although *Hsd11b1* mRNA levels were

low in mouse islets compared with liver and muscle, it was still detectable ($\Delta Ct = 7.33 \pm 1.80$) (Supplementary Fig. 5A). Moreover, *Hsd11b1* mRNA abundance was 55–75% lower in islets from animals expressing a single copy of *Hsd11b1* and undetectable in those deleted for both alleles (Supplementary Fig. 5B), as assessed by specific TaqMan assays. Quantification of *HSD11B1* mRNA revealed similar levels in human and mouse islets, with expression an order of magnitude lower than in human subcutaneous and omental adipose tissue (Supplementary Fig. 5C), a major site of enzyme activity and steroid reactivation (31).

Hsd11b1 Deletion Reverses the Effects of Glucocorticoids on β -Cell Ca^{2+} and cAMP Signaling

As expected, both 11-DHC and corticosterone impaired cytosolic Ca^{2+} fluxes in β -cells residing within islets from *Hsd11b1*^{+/-} animals (Fig. 5A–D and Supplementary Fig. 6A and B). However, deletion of *Hsd11b1* throughout the islet reversed these effects, with 11-DHC and corticosterone no longer able to suppress Ca^{2+} rises in response to glucose or glucose + KCl (Fig. 5E–H and Supplementary Fig. 6C and D). This suggests that local regulation of glucocorticoid activity in the islet may mediate the effects of 11-DHC and corticosterone on β -cell Ca^{2+} fluxes. 11-DHC was able to significantly elevate cAMP responses to glucose in *Hsd11b1*^{+/-} (Fig. 6A–D and Supplementary Fig. 7A) but not *Hsd11b1*^{-/-} islets (Fig. 6E–H and Supplementary Fig. 7B). However, corticosterone still improved cAMP responses to glucose, even after deletion of *Hsd11b1* (Fig. 6A–H and Supplementary Fig. 7A and B). Glucose-stimulated insulin secretion was significantly higher in corticosterone- versus control- or 11-DHC-treated *Hsd11b1*^{-/-} islets (Fig. 6I), consistent with the Ca^{2+} and cAMP results. Similarly, quantitative real-time PCR analyses revealed upregulation of *Adcy1* expression by corticosterone but not by 11-DHC in *Hsd11b1*^{-/-} islets (Fig. 6J and K). Ca^{2+} responses to glucose, glucose + KCl, and KCl were not significantly decreased by 11-DHC (Fig. 7A–F and Supplementary Fig. 8A and B) in islets pretreated with RU486. Similarly, corticosterone was unable to impair Ca^{2+} responses to glucose in RU486-treated islets (Fig. 7E and Supplementary Fig. 8C and D), although Ca^{2+} responses to glucose + KCl were unaffected (Fig. 7F). Thus, the inhibitory actions of the glucocorticoids are partly mediated by the GR.

DISCUSSION

We show that corticosterone and cortisol and their less-active precursors 11-DHC and cortisone impair glucose-, glucose + KCl-, and KCl-stimulated ionic fluxes in rodent and human β -cells. However, insulin secretory output is likely preserved because both glucocorticoids upregulate cAMP signals to increase insulin granule number at the membrane. Invoking a critical role for glucocorticoid interconversion, the effects of 11-DHC could be prevented after islet-wide deletion of *Hsd11b1*. Thus, an enzyme-assisted steroid-regulated feedback loop maintains insulin secretion in the face of altered β -cell ionic signaling (Fig. 8).

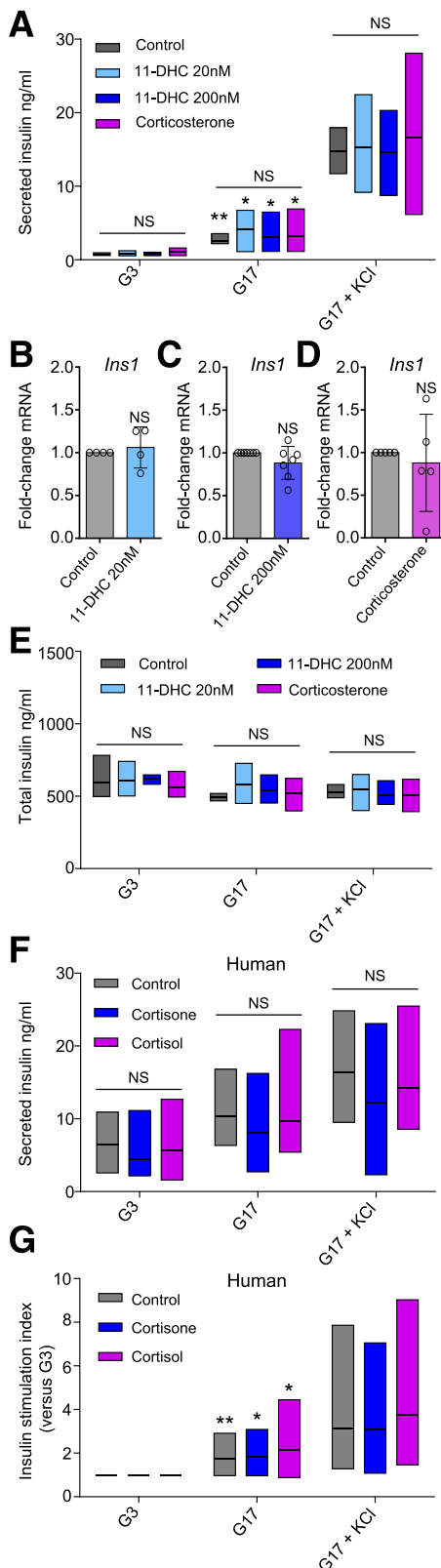


Figure 3—Insulin secretion from islets is maintained in the face of excess glucocorticoid. **A:** Basal, glucose-stimulated, and glucose + KCl-stimulated insulin secretion is unaffected after 48-h treatment of mouse islets with either 11-DHC or corticosterone ($n = 5$ animals). **B–D:** Quantitative real-time PCR analysis of *Ins1* mRNA expression shows no significant changes in response to 11-DHC 20 nmol/L (**B**), 11-DHC 200 nmol/L (**C**), or corticosterone (**D**) ($n = 4$ –7 animals). **E:**

Both corticosterone and 11-DHC have previously been shown to exert inhibitory effects on insulin release (6,7,10,11). However, these studies either used islets from *ob/ob* mice that display highly upregulated *Hsd11b1* expression (6,10) or incubated wild-type islets with glucocorticoid for only 2 h (7,11), which is unlikely to fully compensate for the loss of adrenal input that occurs after islet isolation. Likewise, studies in which glucocorticoids are administered in the drinking water are confounded by insulin resistance and compensatory islet expansion (12). Thus, the effects observed in the current study more likely reflect the cellular/molecular actions of circulating glucocorticoids under normal conditions.

Cytosolic Ca^{2+} responses to glucose were impaired in the presence of either 11-DHC or corticosterone, which was unlikely caused by defects in metabolism and K_{ATP} channel function because glucose-induced ATP/ADP maximal rises were unaffected. However, KCl- and KCl + glucose-induced Ca^{2+} influx as well as VDCC conductance were markedly suppressed, although quantitative real-time PCR analyses of expression levels of the key L-type VDCC subunits showed no differences. Paradoxically, glucocorticoid improved the sustained Ca^{2+} responses to 3 mmol/L glucose + 10 mmol/L KCl. Although this may reflect basal cAMP generation as a result of upregulated *Adcy1*, VDCCs do not open fully under these conditions (Supplementary Table 5), meaning that true defects in their activity are likely to be missed. Indeed, glucocorticoids may induce changes that only restrict Ca^{2+} entry when VDCC open probability increases to support insulin secretion (i.e., 17 mmol/L glucose and/or 30 mmol/L KCl). Ca^{2+} oscillation frequency also was affected, suggesting that glucocorticoids may conceivably target more distal steps in Ca^{2+} flux generation such as intracellular stores (e.g., by depleting them through cAMP sensitization of IP_3 receptors [32]), upregulate ion channels involved in voltage inactivation (i.e., large-conductance Ca^{2+} -activated K^+ channels [33]), or alter glucose-regulated inputs other than cAMP (34). These effects are presumably specific to glucose-stimulated Ca^{2+} rises because responses to the incretin mimetic exendin-4 remained unchanged by glucocorticoid exposure, possibly secondary to PKA-mediated rescue of VDCC function or organellar Ca^{2+} release (35).

Recent RNA sequencing analyses of purified mouse β -cells have shown that *Hsd11b1* mRNA levels are unusually low

Total insulin content is unaffected by 11-DHC or corticosterone ($n = 3$ animals). **F:** Basal, glucose-stimulated, and glucose + KCl-stimulated insulin secretion is unaffected after 48-h treatment of human islets with either cortisone 200 nmol/L or cortisol 20 nmol/L ($n = 3$ donors). **G:** As for **F**, but stimulation index to better account for differences in basal secretion between islet batches from the various isolation centers. Corticosterone was applied at 20 nmol/L for 48 h. KCl was applied at 10 mmol/L. Unless otherwise stated, data are mean \pm SD or range. * $P < 0.05$, ** $P < 0.01$ by Student *t* test, one-way ANOVA (Bonferroni post hoc test), or two-way ANOVA. G3, 3 mmol/L glucose; G17, 17 mmol/L glucose; NS, nonsignificant.

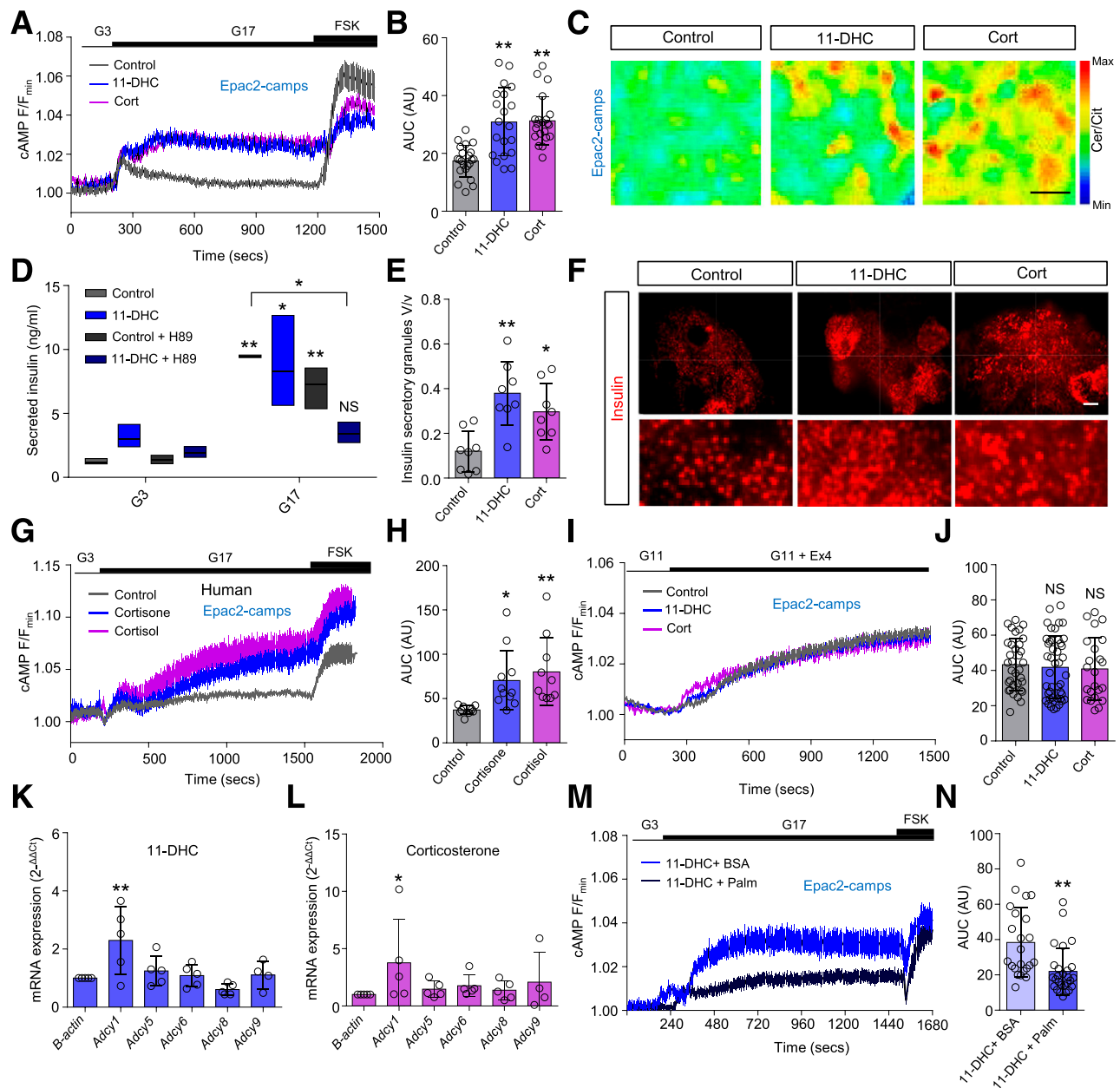


Figure 4—Glucocorticoids potentiate cAMP signaling. **A:** Both 11-DHC and corticosterone amplify glucose-stimulated cAMP generation as measured online by using the biosensor Epac2-camps (forskolin [FSK] positive control; mean \pm SEM traces shown; $n = 20$ –24 islets from five animals). **B:** Summary bar graph showing significant effects of either glucocorticoid on the AUC of cAMP responses to glucose. **C:** Representative images of FRET responses in control-, 11-DHC-, and corticosterone-treated β -cells expressing Epac2-camps (scale bar = 10 μ m). **D:** Inhibition of PKA decreases glucose-stimulated insulin secretion in the presence of 11-DHC but not control (mean and range shown; $n = 3$ animals). **E:** 11-DHC and corticosterone increase the fraction of the cell membrane occupied by insulin granules (V/v). **F:** Representative structured illumination microscopy images showing insulin granules in control-, 11-DHC-, and corticosterone-treated islets ($n = 8$ cells from three animals; scale bar = 5 μ m; bottom panel shows zoom-in). **G:** Cortisone and cortisol augment glucose-stimulated cAMP generation in human islets (mean \pm SEM traces shown). **H:** As for **G**, but summary bar graph showing AUC of cAMP responses to glucose ($n = 10$ –11 islets from three donors). **I:** Glucocorticoid does not affect cAMP responses to extendin-4 (Ex4) 10 nmol/L ($n = 24$ –46 islets from four animals). **J:** As for **I**, but summary bar graph showing AUC of cAMP responses. **K and L:** Relative (fold-change) expression levels of *Adcy1*, -5, -6, -8, and -9 in 11-DHC- (**K**) and corticosterone (**L**)-treated islets ($n = 4$ –5 animals). **M:** Palmitate (Palm) but not BSA control prevents 11-DHC from augmenting cAMP responses to glucose (traces represent mean \pm SEM; $n = 23$ –27 islets from four animals). **N:** As for **M**, but summary bar graph showing AUC of cAMP responses. 11-DHC and corticosterone were applied for 48 h at 200 nmol/L and 20 nmol/L, respectively. Unless otherwise stated, data are mean \pm SD. * $P < 0.05$, ** $P < 0.01$ by Student *t* test or one-way ANOVA (with Bonferroni or Tukey post hoc test). AU, arbitrary unit; Cer/Cit, cerulean/citrine; Cort, corticosterone; G3, 3 mmol/L glucose; G11, 11 mmol/L glucose; G17, 17 mmol/L glucose; max, maximum; min, minimum; NS, nonsignificant.

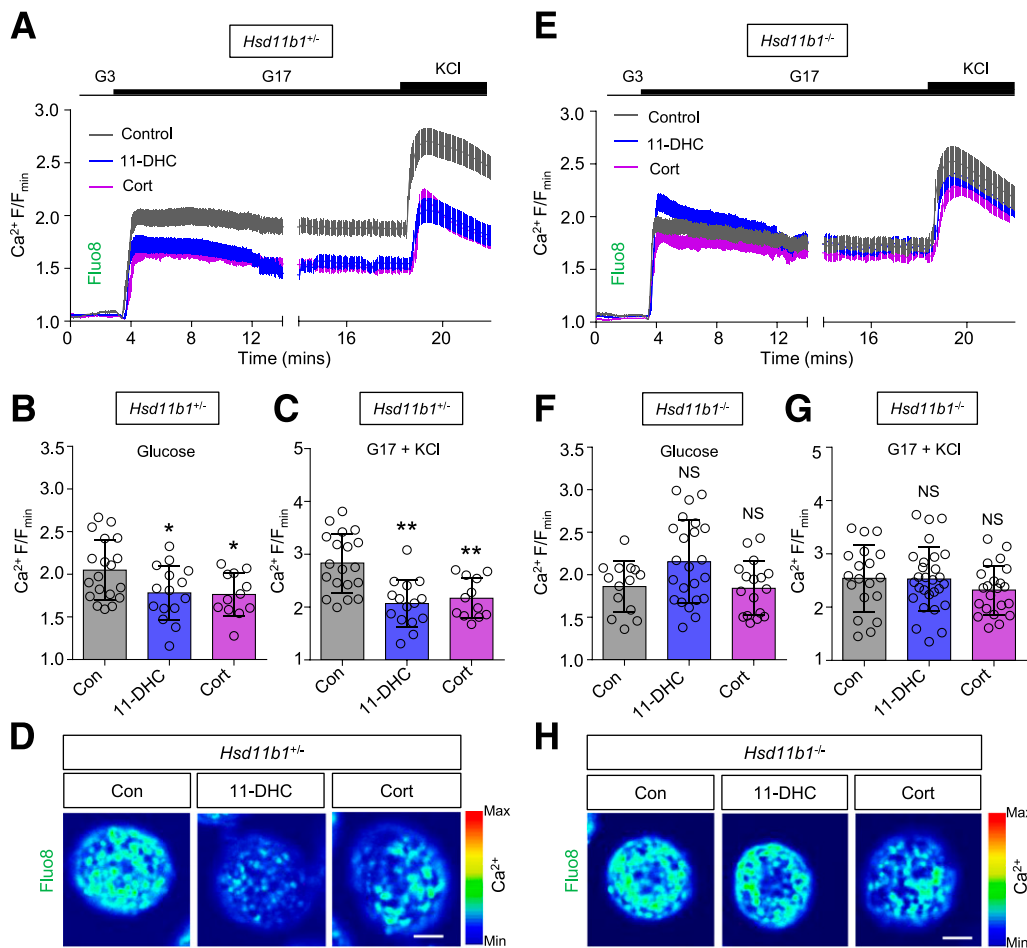


Figure 5—Deletion of *Hsd11b1* reverses the effects of glucocorticoids on Ca^{2+} signaling. **A**: Mean intensity-over-time traces showing a reduction in glucose- and glucose + KCl-stimulated Ca^{2+} rises in *Hsd11b1*^{+/−} islets treated for 48 h with 11-DHC or corticosterone ($n = 15$ – 19 islets from three animals). **B** and **C**: As for **A**, but summary bar graphs showing the amplitude of Ca^{2+} responses to glucose (**B**) and glucose + KCl (**C**). **D**: Representative maximum intensity projection images showing impaired glucose-stimulated Ca^{2+} rises in 11-DHC- and corticosterone- vs. control-treated *Hsd11b1*^{+/−} islets (scale bar = $20\ \mu\text{m}$) (images cropped to show a single islet). **E**: Mean \pm SEM intensity-over-time traces showing intact glucose- and glucose + KCl-stimulated Ca^{2+} rises in *Hsd11b1*^{−/−} islets treated for 48 h with 11-DHC or corticosterone ($n = 19$ – 28 islets from three animals). **F** and **G**: As for **E**, but summary bar graphs showing the amplitude of Ca^{2+} responses to glucose (**F**) and glucose + KCl (**G**). **H**: Representative maximum intensity projection images showing similar glucose-stimulated Ca^{2+} rises in 11-DHC- and corticosterone- vs. control-treated *Hsd11b1*^{−/−} islets (scale bar = $20\ \mu\text{m}$) (images cropped to show a single islet). 11-DHC and corticosterone were applied for 48 h at $200\ \text{nmol/L}$ and $20\ \text{nmol/L}$, respectively. KCl was applied at $10\ \text{mmol/L}$. Unless otherwise stated, data are mean \pm SD. * $P < 0.05$, ** $P < 0.01$ by one-way ANOVA (Bonferroni post hoc test). Con, control; Cort, corticosterone; G3, $3\ \text{mmol/L}$ glucose; G17, $17\ \text{mmol/L}$ glucose; max, maximum; min, minimum; NS, nonsignificant.

in these and other islet endocrine cells (i.e., it is an islet disallowed gene) (36). Likewise, *HSD11B1* levels were low in human β - and α -cells (37). These findings contrast with reports that protein expression colocalizes with glucagon or insulin in rodent islets depending on the antibody used (7,38). The reasons for these discrepancies are unclear, but in the current study, specific TaqMan assays showed consistently detectable mRNA levels in both rodent and human islets. Moreover, 11-DHC effects could be prevented in global *Hsd11b1*^{−/−} islets in which mRNA was largely absent and *HSD11B1* expression in human islets is only an order of magnitude lower than in adipose tissue, a major site for steroid reactivation after the liver (31). Thus, 11-DHC likely affects β -cell function in a paracrine manner,

possibly through the actions of HSD11B1 in nonendocrine islet cell types (e.g., endothelial cells where expression levels are higher [37]). This may form the basis of an adaptive mechanism to prevent the build-up of high local corticosterone/cortisol concentrations. Together, these data highlight the importance of the islet context for the regulation of insulin secretion and underline the requirement to consider cell-cell cross talk when assessing the functional consequences of β -cell gene disallowance.

Global deletion of *Hsd11b1* prevented the effects of 11-DHC on ionic and cAMP fluxes, as expected, suggesting that local regulation of glucocorticoid activity is important for β -cell function. However, corticosterone was unable to impair Ca^{2+} responses in *Hsd11b1*^{−/−} islets, whereas

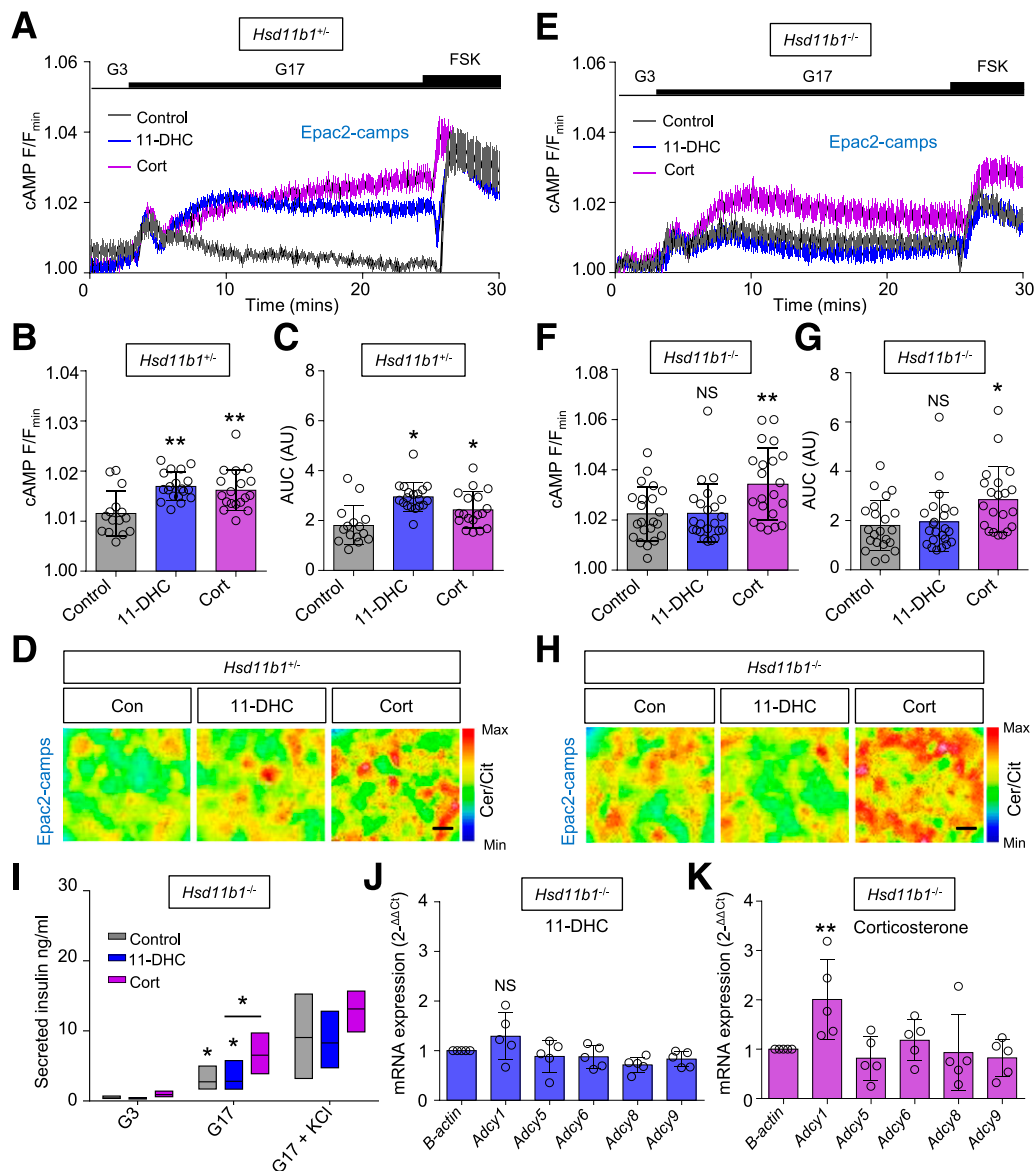


Figure 6—Deletion of *Hsd11b1* reverses the effects of 11-DHC on cAMP signaling. **A:** Mean \pm SEM intensity-over-time traces showing cAMP responses to glucose in 11-DHC- and corticosterone-treated *Hsd11b1*^{+/−} islets (forskolin [FSK] positive control; $n = 15$ –19 islets from three animals). **B** and **C:** As for **A**, but summary bar graphs showing the amplitude (**B**) and AUC (**C**) of cAMP responses. **D:** Representative images of cAMP responses to glucose in control-, 11-DHC-, or corticosterone-treated *Hsd11b1*^{+/−} islets expressing Epac2-camps (scale bar = 10 μ m). **E:** Mean \pm SEM intensity-over-time traces showing that cAMP responses to glucose are potentiated by corticosterone but not 11-DHC in *Hsd11b1*^{−/−} islets ($n = 22$ –23 islets from three animals). **F** and **G:** As for **E**, but summary bar graphs showing the amplitude (**F**) and AUC (**G**) of cAMP responses. **H:** Representative images of cAMP responses to glucose in control-, 11-DHC-, and corticosterone-treated *Hsd11b1*^{−/−} islets expressing Epac2-camps (scale bar = 10 μ m). **I:** Insulin secretion in response to glucose is significantly improved in corticosterone- vs. control- and 11-DHC-treated *Hsd11b1*^{−/−} islets ($n = 4$ animals). **J** and **K:** Relative (fold-change) expression levels of *Adcy1*, *-5*, *-6*, *-8*, and *-9* in 11-DHC- (**J**) and corticosterone (**K**)-treated *Hsd11b1*^{−/−} islets ($n = 5$ animals). 11-DHC and corticosterone were applied for 48 h at 200 nmol/L and 20 nmol/L, respectively. KCl was applied at 10 mmol/L. Unless otherwise stated, data are mean \pm S.D. * $P < 0.05$, ** $P < 0.01$ by Student *t* test or one-way ANOVA (Bonferroni post hoc test). AU, arbitrary unit; Cer/Cit, cerulean/citrine; Con, control; Cort, corticosterone; G3, 3 mmol/L glucose; G17, 17 mmol/L glucose; max, maximum; min, minimum; NS, nonsignificant.

potentiation of cAMP remained intact. Together, these observations raise the possibility that corticosterone may undergo substantial oxidation to 11-DHC through HSD11B2 (37), with local concentrations dropping below the threshold for suppression of Ca²⁺ but not cAMP after *Hsd11b1* knockout. Although previous studies have shown that a single *Hsd11b1* allele is sufficient for full enzymatic activity

(39), additional studies are required to determine whether this is also the case in islets.

Consistent with upregulated cAMP signaling, an increase in the number of submembrane insulin granules was observed in glucocorticoid-treated islets. cAMP has been shown to recruit nondocked insulin granules to the membrane as well as to increase the size of the readily-releasable

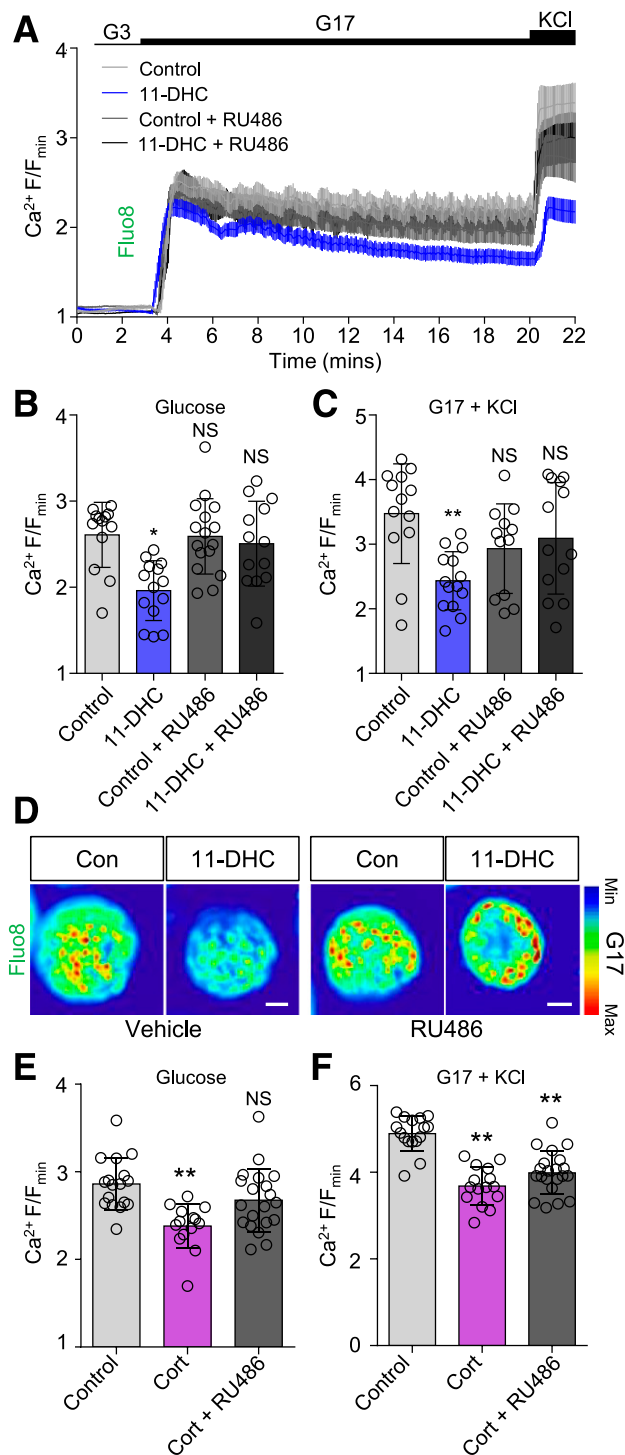


Figure 7—11-DHC effects are mediated through the GR. **A**: The GR antagonist RU486 prevents the suppressive effects of 11-DHC on glucose- and glucose + KCl-stimulated Ca^{2+} signals (mean \pm SEM traces shown; $n = 12$ –13 islets from four animals). **B** and **C**: As for **A**, but summary bar graphs showing that 11-DHC does not affect Ca^{2+} responses to glucose (**B**) or glucose + KCl (**C**) in RU486-treated islets. **D**: Representative maximum intensity projection images showing impaired Ca^{2+} rises in 11-DHC-treated islets, which can be reversed by using the GR antagonist RU486 (scale bar = 20 μm) (images cropped to show a single islet). **E**: RU486 blocks the effects of corticosterone on Ca^{2+} responses to glucose ($n = 14$ –17 islets from six animals). **F**: As for **E**, but RU486 is unable to significantly affect Ca^{2+} responses to glucose + KCl in corticosterone-treated islets ($n = 14$ –17 islets from

granule pool through Epac2 and PKA (40,41), and this may account for the intact secretory responses to glucose and KCl. The exact mechanisms by which 11-DHC and corticosterone boost cAMP signaling are unknown but likely involve specific adenylate cyclases because *Adcy1* gene expression was increased in 11-DHC- and corticosterone-treated islets compared with controls. Moreover, palmitate, which downregulates *Adcy9* and impairs cAMP responses to glucose (29), prevented 11-DHC from increasing cAMP levels. Although *Adcy9* mRNA expression was not significantly affected by glucocorticoid, other mechanisms can account for cAMP generation, including organization of the enzyme into microdomains (42). Pertinently, knockdown of *Adcy1* and *Adcy9* has been shown to reduce glucose-stimulated cAMP rises and insulin secretion in β -cells (29,43). Additional studies thus are warranted in glucocorticoid-treated *Adcy1*- and *Adcy9*-null islets. Upregulated cAMP signaling may represent a protective mechanism that is disrupted by free fatty acids to induce β -cell failure/decompensation in the face of excess glucocorticoid. Of note, endogenous elevation of glucocorticoids leads to dyslipidemia as a result of lipolysis, de novo fatty acid production/turnover, and hepatic fat accumulation (44).

In mouse islets, cAMP responses to glucose have been shown to be oscillatory (29), albeit noisier than those in MIN6/INS-1E cells (45). However, the latter study used total internal reflection fluorescence microscopy to study submembrane cAMP responses, whose changes may be larger and more dynamic than those recorded throughout the cytosol (46). Similar studies that used epifluorescence techniques showed nonoscillatory cAMP increases in response to high glucose concentrations (47). Thus, additional studies are required to investigate the impact of glucocorticoids on cAMP oscillations, which were not detectable at the axial resolutions used here. Although ATP/ADP responses were oscillatory in single islets, a transient dip was present after introduction of high glucose. This has also been seen in previous studies (19) and may reflect net ATP consumption secondary to Ca^{2+} transporter activity (48), glucokinase activity (49) and the initial steps of exocytosis (50), or an uncoupling effect of highly elevated Ca^{2+} levels on mitochondrial function (21). Although similar results were seen with luciferase-based ATP measures, a change in intracellular pH and Perceval intensity cannot be excluded.

In summary, we have identified a novel mechanism by which glucocorticoids maintain β -cell function in rodent and human β -cells through engagement of parallel cAMP

six animals). 11-DHC and corticosterone were applied for 48 h at 200 nmol/L and 20 nmol/L, respectively. KCl was applied at 10 mmol/L. Unless otherwise stated, data are mean \pm SD. * $P < 0.05$, ** $P < 0.01$ by one-way ANOVA (Bonferroni post hoc test). Islets were pretreated with 1 $\mu\text{mol/L}$ RU486. Con, control; Cort, corticosterone; G3, 3 mmol/L glucose; G17, 17 mmol/L glucose; max, maximum; min, minimum; NS, nonsignificant.

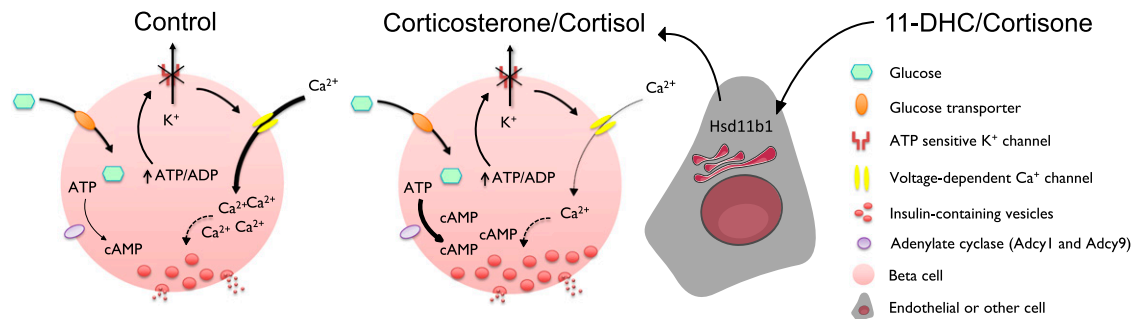


Figure 8—Glucocorticoids impair K_{ATP} -independent signals to reduce ionic fluxes in glucose-stimulated β -cells. This is further exacerbated by HSD11B1, which increases availability of more active glucocorticoid (11-DHC/cortisone \rightarrow corticosterone/cortisol) in a paracrine manner. However, insulin secretion is preserved because glucocorticoids reprogram the β -cell signaling cassette toward a cAMP phenotype most likely through upregulation of specific Adcy isoforms.

pathways. Failure of this protective feedback loop may contribute to impaired insulin release during states of glucocorticoid excess (e.g., Cushing syndrome).

Acknowledgments. The authors thank Gary Yellen (Harvard University) for providing the plasmid for Perceval. They also thank Dr. Jocelyn E. Manning Fox and Patrick E. MacDonald for provision of human islets through the Alberta Diabetes Institute IsletCore at the University of Alberta with the assistance of the Human Organ Procurement and Exchange program, Trillium Gift of Life Network, and other Canadian organ procurement organizations. The authors are grateful to the European Consortium for Islet Transplantation (ECIT), which was supported by JDRF award 31-2008-416 (ECIT Islet for Basic Research program).

Funding. N.C.V. and D.A.J. were supported by National Institutes of Health grant R01-DK-097392 and American Diabetes Association grant 1-17-IBS-024. P.M. and M.B. were supported by the Innovative Medicine Initiative Joint Undertaking under grant agreement no. 155005 (iMiDiA), resources of which comprised financial contributions from the European Union's Seventh Framework Programme (FP7/2007-2013) and in-kind contributions from European Federation of Pharmaceutical Industries and Associations companies, and by the Italian Ministry of Education, University and Research (PRIN 2010-2012). L.P. provided human islets through collaboration with the Diabetes Research Institute, San Raffaele Scientific Institute (Milan, Italy), within the European islet distribution program for basic research supported by JDRF (1-RSC-2014-90-1-X). G.A.R. was supported by Wellcome Trust Senior Investigator (WT098424AIA) and Royal Society Wolfson Research Merit awards and by Medical Research Council (MRC) Programme (MR/J0003042/1), Biological and Biotechnology Research Council (BB/J015873/1), and Diabetes UK project (11/0004210) grants. G.A.R. and D.J.H. were supported by an MRC project grant (MR/N00275X/1). G.G.L. was supported by a Wellcome Trust Senior Research Fellowship (104612/Z/14/Z). D.J.H. was supported by a Diabetes UK R.D. Lawrence grant (12/0004431), European Foundation for the Study of Diabetes (EFSD)/Novo Nordisk Rising Star Fellowship, and Wellcome Trust Institutional Support Award. This project has received funding from the European Research Council under the European Union's Horizon 2020 research and innovation program (Starting Grant 715884 to D.J.H.).

Duality of Interest. No potential conflicts of interest relevant to this article were reported.

Author Contributions. N.H.F.F. conceived and devised the study, performed the experiments, and analyzed data. C.L.D., Y.S.E., N.C.V., and D.A.J. performed experiments and analyzed data. P.M., M.B., R.N., and L.P. isolated and provided human islets. G.A.R. provided reagents. G.G.L. provided reagents and analyzed data. D.J.H. supervised the research, conceived and devised the study, performed analyses, and wrote the manuscript with input from all authors. D.J.H. is the guarantor of this work and, as such, had full access to all the data in the study and takes responsibility for the integrity of the data and the accuracy of the data analysis.

Prior Presentation. Parts of this study were presented in abstract form at the 53rd Annual Meeting of the European Association for the Study of Diabetes, Lisbon, Portugal, 11–15 September 2017.

References

- Andrews RC, Walker BR. Glucocorticoids and insulin resistance: old hormones, new targets. *Clin Sci (Lond)* 1999;96:513–523
- Seckl JR, Walker BR. Minireview: 11 β -hydroxysteroid dehydrogenase type 1—a tissue-specific amplifier of glucocorticoid action. *Endocrinology* 2001;142:1371–1376
- Ogawa A, Johnson JH, Ohneda M, et al. Roles of insulin resistance and beta-cell dysfunction in dexamethasone-induced diabetes. *J Clin Invest* 1992;90:497–504
- Delaunay F, Khan A, Cintra A, et al. Pancreatic beta cells are important targets for the diabetogenic effects of glucocorticoids. *J Clin Invest* 1997;100:2094–2098
- Lambillotte C, Gilon P, Henquin JC. Direct glucocorticoid inhibition of insulin secretion. An in vitro study of dexamethasone effects in mouse islets. *J Clin Invest* 1997;99:414–423
- Davani B, Khan A, Hult M, et al. Type 1 11beta -hydroxysteroid dehydrogenase mediates glucocorticoid activation and insulin release in pancreatic islets. *J Biol Chem* 2000;275:34841–34844
- Swali A, Walker EA, Lavery GG, Tomlinson JW, Stewart PM. 11Beta-hydroxysteroid dehydrogenase type 1 regulates insulin and glucagon secretion in pancreatic islets. *Diabetologia* 2008;51:2003–2011
- Koizumi M, Yada T. Sub-chronic stimulation of glucocorticoid receptor impairs and mineralocorticoid receptor protects cytosolic Ca^{2+} responses to glucose in pancreatic beta-cells. *J Endocrinol* 2008;197:221–229
- Gremlich S, Roduit R, Thorens B. Dexamethasone induces posttranslational degradation of GLUT2 and inhibition of insulin secretion in isolated pancreatic beta cells. Comparison with the effects of fatty acids. *J Biol Chem* 1997;272:3216–3222
- Ortsäter H, Alberts P, Warpman U, Engblom LOM, Abrahmsén L, Bergsten P. Regulation of 11 β -hydroxysteroid dehydrogenase type 1 and glucose-stimulated insulin secretion in pancreatic islets of Langerhans. *Diabetes Metab Res Rev* 2005;21:359–366
- Turban S, Liu X, Ramage L, et al. Optimal elevation of β -cell 11 β -hydroxysteroid dehydrogenase type 1 is a compensatory mechanism that prevents high-fat diet-induced β -cell failure. *Diabetes* 2012;61:642–652
- Rafacho A, Marroquí L, Taboga SR, et al. Glucocorticoids in vivo induce both insulin hypersecretion and enhanced glucose sensitivity of stimulus-secretion coupling in isolated rat islets. *Endocrinology* 2010;151:85–95
- Stamateris RE, Sharma RB, Hollern DA, Alonso LC. Adaptive β -cell proliferation increases early in high-fat feeding in mice, concurrent with metabolic changes, with induction of islet cyclin D2 expression. *Am J Physiol Endocrinol Metab* 2013;305:E149–E159

14. Gesina E, Tronche F, Herrera P, et al. Dissecting the role of glucocorticoids on pancreas development. *Diabetes* 2004;53:2322–2329
15. Shen CN, Seckl JR, Slack JM, Tosh D. Glucocorticoids suppress beta-cell development and induce hepatic metaplasia in embryonic pancreas. *Biochem J* 2003;375:41–50
16. Guo S, Dai C, Guo M, et al. Inactivation of specific β cell transcription factors in type 2 diabetes. *J Clin Invest* 2013;123:3305–3316
17. Kotelevtsev Y, Holmes MC, Burchell A, et al. 11 β -hydroxysteroid dehydrogenase type 1 knockout mice show attenuated glucocorticoid-inducible responses and resist hyperglycemia on obesity or stress. *Proc Natl Acad Sci U S A* 1997;94:14924–14929
18. Lyon J, Manning Fox JE, Spigelman AF, et al. Research-focused isolation of human islets from donors with and without diabetes at the Alberta Diabetes Institute IsletCore. *Endocrinology* 2016;157:560–569
19. Hodson DJ, Tarasov AI, Gimeno Brias S, et al. Incretin-modulated beta cell energetics in intact islets of Langerhans. *Mol Endocrinol* 2014;28:860–871
20. Hodson DJ, Mitchell RK, Marselli L, et al. ADCY5 couples glucose to insulin secretion in human islets. *Diabetes* 2014;63:3009–3021
21. Li J, Shuai HY, Gylfe E, Tengholm A. Oscillations of sub-membrane ATP in glucose-stimulated beta cells depend on negative feedback from Ca(2+). *Diabetologia* 2013;56:1577–1586
22. Zhu L, Almaça J, Dadi PK, et al. β -Arrestin-2 is an essential regulator of pancreatic β -cell function under physiological and pathophysiological conditions. *Nat Commun* 2017;8:14295
23. Hodson DJ, Mitchell RK, Bellomo EA, et al. Lipotoxicity disrupts incretin-regulated human β cell connectivity. *J Clin Invest* 2013;123:4182–4194
24. Hattlapatka K, Willenborg M, Rustenbeck I. Plasma membrane depolarization as a determinant of the first phase of insulin secretion. *Am J Physiol Endocrinol Metab* 2009;297:E315–E322
25. Piccand J, Strasser P, Hodson DJ, et al. Rfx6 maintains the functional identity of adult pancreatic β cells. *Cell Reports* 2014;9:2219–2232
26. Berg J, Hung YP, Yellen G. A genetically encoded fluorescent reporter of ATP:ADP ratio. *Nat Methods* 2009;6:161–166
27. Rutter GA, Pullen TJ, Hodson DJ, Martinez-Sanchez A. Pancreatic β -cell identity, glucose sensing and the control of insulin secretion. *Biochem J* 2015;466:203–218
28. Holz GG, Kang G, Harbeck M, Roe MW, Chepurny OG. Cell physiology of cAMP sensor Epac. *J Physiol* 2006;577:5–15
29. Tian G, Sol ER, Xu Y, Shuai H, Tengholm A. Impaired cAMP generation contributes to defective glucose-stimulated insulin secretion after long-term exposure to palmitate. *Diabetes* 2015;64:904–915
30. Morgan SA, McCabe EL, Gathercole LL, et al. 11 β -HSD1 is the major regulator of the tissue-specific effects of circulating glucocorticoid excess. *Proc Natl Acad Sci U S A* 2014;111:E2482–E2491
31. Tomlinson JW, Moore JS, Clark PM, Holder G, Shakespeare L, Stewart PM. Weight loss increases 11 β -hydroxysteroid dehydrogenase type 1 expression in human adipose tissue. *J Clin Endocrinol Metab* 2004;89:2711–2716
32. Liu YJ, Grapengiesser E, Gylfe E, Hellman B. Crosstalk between the cAMP and inositol trisphosphate-signalling pathways in pancreatic beta-cells. *Arch Biochem Biophys* 1996;334:295–302
33. Jacobson DA, Mendez F, Thompson M, Torres J, Cochet O, Philipson LH. Calcium-activated and voltage-gated potassium channels of the pancreatic islet impart distinct and complementary roles during secretagogue induced electrical responses. *J Physiol* 2010;588:3525–3537
34. Henquin JC. Triggering and amplifying pathways of regulation of insulin secretion by glucose. *Diabetes* 2000;49:1751–1760
35. Ammälä C, Ashcroft FM, Rorsman P. Calcium-independent potentiation of insulin release by cyclic AMP in single beta-cells. *Nature* 1993;363:356–358
36. Pullen TJ, Huisin MO, Rutter GA. Analysis of purified pancreatic islet beta and alpha cell transcriptomes reveals 11 β -hydroxysteroid dehydrogenase (Hsd11b1) as a novel disallowed gene. *Front Genet* 2017;8:41
37. Segerstolpe Å, Palasantza A, Eliasson P, et al. Single-cell transcriptome profiling of human pancreatic islets in health and type 2 diabetes. *Cell Metab* 2016;24:593–607
38. Chowdhury S, Grimm L, Gong YJ, et al. Decreased 11 β -hydroxysteroid dehydrogenase 1 level and activity in murine pancreatic islets caused by insulin-like growth factor I overexpression. *PLoS One* 2015;10:e0136656
39. Abrahams L, Semjonous NM, Guest P, et al. Biomarkers of hypothalamic-pituitary-adrenal axis activity in mice lacking 11 β -HSD1 and H6PDH. *J Endocrinol* 2012;214:367–372
40. Shibasaki T, Takahashi H, Miki T, et al. Essential role of Epac2/Rap1 signaling in regulation of insulin granule dynamics by cAMP. *Proc Natl Acad Sci U S A* 2007;104:19333–19338
41. Kaihara KA, Dickson LM, Jacobson DA, et al. β -Cell-specific protein kinase A activation enhances the efficiency of glucose control by increasing acute-phase insulin secretion. *Diabetes* 2013;62:1527–1536
42. Cooper DM. Regulation and organization of adenylyl cyclases and cAMP. *Biochem J* 2003;375:517–529
43. Kitaguchi T, Oya M, Wada Y, Tsuboi T, Miyawaki A. Extracellular calcium influx activates adenylyl cyclase 1 and potentiates insulin secretion in MIN6 cells. *Biochem J* 2013;450:365–373
44. Arnaldi G, Scandali VM, Trementino L, Cardinaletti M, Appolloni G, Boscaro M. Pathophysiology of dyslipidemia in Cushing's syndrome. *Neuroendocrinology* 2010;92(Suppl. 1):86–90
45. Idevall-Hagren O, Barg S, Gylfe E, Tengholm A. cAMP mediators of pulsatile insulin secretion from glucose-stimulated single beta-cells. *J Biol Chem* 2010;285:23007–23018
46. Dyachok O, Idevall-Hagren O, Sätgetorp J, et al. Glucose-induced cyclic AMP oscillations regulate pulsatile insulin secretion. *Cell Metab* 2008;8:26–37
47. Landa LR Jr, Harbeck M, Kaihara K, et al. Interplay of Ca²⁺ and cAMP signaling in the insulin-secreting MIN6 beta-cell line. *J Biol Chem* 2005;280:31294–31302
48. Tarasov AI, Griffiths EJ, Rutter GA. Regulation of ATP production by mitochondrial Ca(2+). *Cell Calcium* 2012;52:28–35
49. Kamata K, Mitsuya M, Nishimura T, Eiki J, Nagata Y. Structural basis for allosteric regulation of the monomeric allosteric enzyme human glucokinase. *Structure* 2004;12:429–438
50. Detimary P, Gilon P, Nenquin M, Henquin JC. Two sites of glucose control of insulin release with distinct dependence on the energy state in pancreatic B-cells. *Biochem J* 1994;297:455–461